Conformation-Specific Recognition of Carcinogen−DNA Adduct in Escherichia coli Nucleotide Excision Repair

ARTICLE *in* CHEMICAL RESEARCH IN TOXICOLOGY · FEBRUARY 2007

Impact Factor: 3.53 · DOI: 10.1021/tx600273h · Source: PubMed

4 AUTHORS, INCLUDING:

Steven Michael Shell
University of Virginia
20 PUBLICATIONS **620** CITATIONS
SEE PROFILE

Yue Zou
East Tennessee State University
67 PUBLICATIONS **2,075** CITATIONS
SEE PROFILE

Communications

Conformation-Specific Recognition of Carcinogen−DNA Adduct in *Escherichia coli* Nucleotide Excision Repair

Srinivasarao Meneni,[†] Steven M. Shell,[‡] Yue Zou,[‡] and Bongsup P. Cho*[,†]

Department of Biomedical and Pharmaceutical Sciences, College of Pharmacy, University of Rhode Island, 41 Lower College Road, Kingston, Rhode Island 02881, and Department of Biochemistry and Molecular Biology, Quillen College of Medicine, East Tennessee State University, Johnson City, Tennessee 37614

Received October 13, 2006

We report a systematic and quantitative structure−function relationship study of the major *N*-[deoxyguanosin-8-yl]-2-aminofluorene adduct (AF) derived from the prototype carcinogen 2-aminofluorene and its derivatives. The AF adduct is known to exist in two distinct conformational motifs, depending upon the location of the hydrophobic fluorine moiety: major groove binding "B type" (B) conformation (AF-dG$_{anti}$) and base-displaced "stacked" (S) conformation (AF-dG$_{syn}$). The AF-induced S/B conformational heterogeneity is sequence-dependent and follows a typical two-site dynamic chemical exchange. The population of S conformation decreases in the order of 3′-G > A ≫ C > T, indicating the importance of the purine flanking bases in promoting the stacking structure. Line-shape analysis showed that the S/B interconversion energy barriers ($\Delta G^{\ddagger}$) are in the narrow 14−16 kcal/mol range. The energy differences of the two conformers are relatively small (<0.5 kcal/mol), suggesting a possibility for a facile adduct conformation switch in the active site of a polymerase. The S/B equilibrium modulates the efficiency of *Escherichia coli* UvrABC-based nucleotide excision repair (NER) in a conformation-specific manner. The ^{19}F NMR/NER results indicate greater repair susceptibility for the base-displaced S conformer, which lacks a Watson−Crick base pair at the lesion site. These findings represent the first of its kind quantitative structure−function work relating NER activity to a specific adduct conformer and will lead to a better understanding of how bulky DNA adducts are accommodated by the repair protein.

Introduction

Genetic degeneration is linked closely with maintenance of DNA integrity and gene function (*1*). DNA adduct formation is a signature hallmark for mutation, leading to the initiation of chemical carcinogenesis (*2*). The complexity of adduct structures, however, has impeded the elucidation of an unambiguous structure−mutation relationship at the molecular genetic level (*3*, *4*). A case in point is the prototype arylamine carcinogen 2-aminofluorene and its derivatives, which upon activation in vivo, produce two major dG−C8-modified *N*-[deoxyguanosin-8-yl]-2-aminofluorene (AF)[1] and AAF adducts (Figure 1a) (*5*). They exhibit uniquely different mutation and repair activities. Translesional synthesis of the N-deacetylated AF is achieved with high-fidelity polymerases, whereas replication of the bulky AAF requires bypass polymerases (*6*). Nucleotide excision repair (NER) of the two adducts is modulated by base sequences. For example, Mekhovich et al. (*7*) have shown in 1998 that the rate of incision of both AF and AAF adducts in the *Escherichia coli* UvrABC system is significantly faster when they are positioned in the mutation hotspot *Nar*I sequence (5′-GGCG*CC-3′) than when located in a random sequence (5-GATG*ATA-3′). The sequence dependence of NER efficiency has since been well-documented in both bacterial (*8*) and mammalian (*9*) systems and may account for so-called "hot" mutation spots.

Solution NMR studies have shown that AF in fully complementary DNA duplexes adopts a sequence-dependent equilibrium between B and S conformations defined by the glycosidyl configurations (anti and syn, respectively) of the modified dG (Figure 1b) (*4*, *10*, *11)*. In the B conformer, the *anti*-[AF]dG maintains Watson−Crick hydrogen bonds, thereby placing the aminofluorene ring in the major groove. This is contrasted with the aminofluorene moiety of the S conformer, which stacks into the helix with *syn*-[AF]dG. A minor groove binding wedged (W) conformer with *syn*-[AF]dG has also been observed in duplexes where the lesion was mismatched with purine bases (*12*). Interestingly, evidence exists for a similar S/B conformational heterogeneity in the active site of a crystal polymerase (*13*). Here, we report a novel conformation-specific repair study involving the S/B population ratios and NER activities.

Experimental Procedures

Caution: *2-Aminofluorene derivatives are mutagens and a suspected human carcinogen and must be handled with caution.*

Crude desalted oligodeoxynucleotides in 10 μmol scales were obtained from Sigma-Genosys (The Woodlands, TX). All HPLC solvents were purchased from Fisher Inc. (Pittsburgh, PA).

Preparation of FAF-Modified Oligodeoxynucleotides. The FAF-modified oligonucleotides (Figure 1a) were prepared by

* To whom correspondence should be addressed.
[†] University of Rhode Island.
[‡] East Tennessee State University.

[1]Abbreviations: NER, nucleotide excision repair; AF adduct, *N*-[deoxyguanosin-8-yl]-2-aminofluorene; ^{19}F NMR, ^{19}F nuclear magnetic resonance spectroscopy.

10.1021/tx600273h CCC: $37.00
Published on Web 12/29/2006

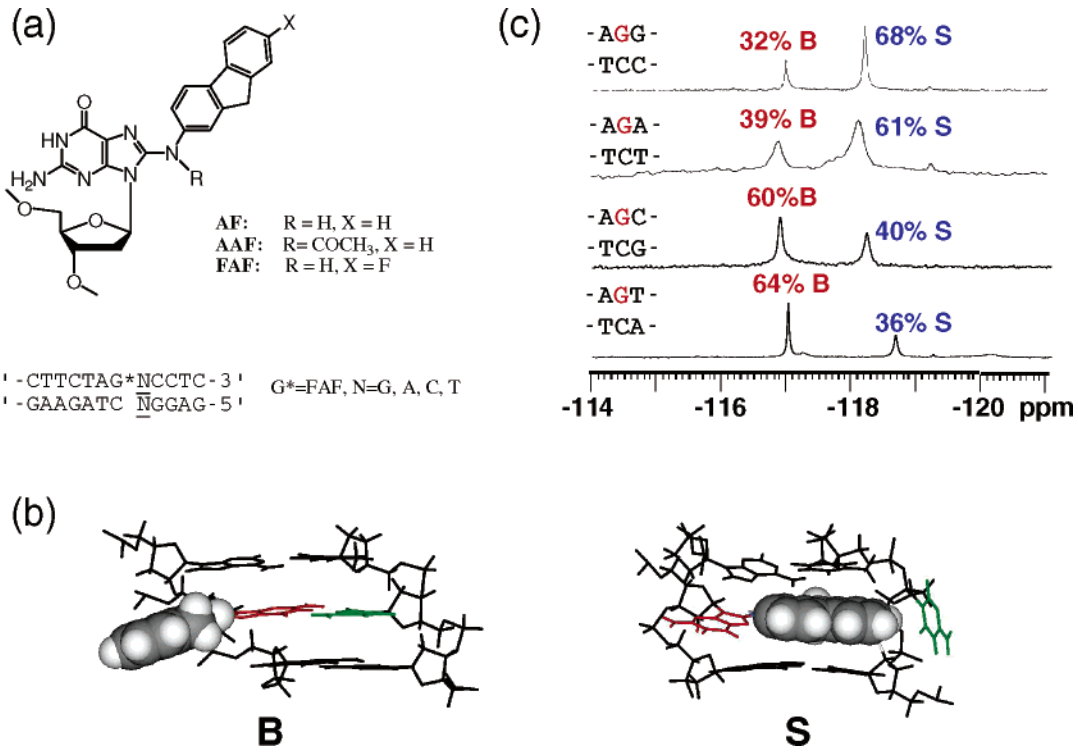

Figure 1. (a) Chemical structures of aminofluorene−DNA adducts and duplex sequences used in this study. (b) The central trimer segments of the B and S conformers of AF-modified DNA (−AG*A− duplex is shown as an example). Views from the major groove. The modified dG and the complementary dC are shown in red and green, respectively, and the AF moiety is highlighted with gray CPK. In the B conformer, anti-[AF]dG maintains Watson−Crick hydrogen bonds, thereby placing the AF ring in the major groove. The AF moiety of the S conformer stacks into the helix with the modified dG in the syn conformation. (c) ^{19}F NMR spectra of the −AG[FAF]*N*− duplex sequences (*N* = G, A, C, T) in a pH 7.0 10%D_2O/90% H_2O phosphate buffer at 20 °C.

treating a desalted oligonucleotide (Sigma-Genosys) with *N*-acetoxy-*N*-(trifluoroacetyl)-7-fluoro-2-aminofluorene (*10*). Each modified oligo was purified by reverse phase HPLC and characterized by UV/enzyme digest/eletrospray mass spectrometry as described previously (*10*, *12*, *14*). The HPLC system consisted of a Hitachi EZChrom Elite system with a L2450 diode array as a detector and a Luna column (10 mm × 150 mm, 5 μm) (Phenomenex, Torrance, CA). The mobile phase system involved a 30 min linear gradient profile of 3−15% acetonitrile/0.1 M ammonium acetate buffer (pH 7.0) with a flow rate of 2.0 mL/min. Approximately 80−100 ods of pure modified oliognucleotides were annealed with appropriate complementary sequences to form fully complementary heteroduplexes and centrifuged through a Millipore Centricon YM-3 centrifugal filter (Yellow, molecular weight cutoff = 3000). The filtered samples were redissolved in a Shigemi NMR tube containing 300 μL of pH 7.0 NMR buffer (10% D_2O/90% H_2O): 100 mM NaCl, 10 mM sodium phosphate, and 100 μM tetrasodium EDTA.

NMR Experiments. All ^{1}H-decoupled ^{19}F NMR results were recorded using a dedicated 5 mm ^{19}F/^{1}H dual probe on a Bruker DPX400 Avance spectrometer operating at 376.5 MHz. Spectra were referenced to $CFCl_3$ by assigning external hexafluorobenzene in C_6D_6 at −164.90 ppm. One-dimensional ^{19}F NMR spectra at various temperatures (5−60 °C) were obtained by collecting 65536 points using a 37664 Hz sweep width and a recycle delay of 1.0 s between acquisitions. A total of 1600 scans were acquired for each spectrum. The spectra were processed by zero-filling, exponential multiplication using 20 Hz line broadening, and Fourier transformation. The peak areas were baseline corrected and integrated using XWIN software (Bruker, Billerica, MA). Two-dimensional NOESY/exchange ^{19}F NMR spectra (*10*) were carried out in the phase-sensitive mode using a NOESY pulse sequence: sweep width, 4529 Hz; number of complex data points in t_2, 1024; number of complex free induction decays in t_1, 256; number of scans, 96; dummy scans, 16; recycle delays, 1.0 s; and mixing time, 400 ms. The data were subjected to sine bell apodization using 2 Hz line broadening in both dimensions and then zero-filled before Fourier transformation of the 1024 × 256 data matrix.

Complete Line Shape Analysis. Initially, the values of frequencies and the S/B population ratios were determined at the slow exchange limit (5 °C). Next, several spectra were recorded at various temperatures between 5 and 60 °C including at coalescence and into the fast exchange region. Finally, the sample was cooled back to the slow exchange limit to ensure that no irreversible process occurred at the higher temperatures. Complete line-shape analysis was carried out using WINDNMR-Pro (version 7.1.6, *J. Chem. Educ*. Software Series; Reich, H. J., University of Wisconsin, Madison, WI) to calculate rate constants (*k*), free energy difference $\Delta G°$ ($-RT\ln K$eq), and the S/B interconversion energy barrier $\Delta G^‡$ (Table 1) (*15*).

Modeling. The solution structure of the AF-intercalated S conformer opposite dC in an 11-mer DNA (*16*) was employed as the starting model for the FAF-modified S conformer. The sequences of NMR-derived structures were adjusted to that of the target 12-mer sequence (CTTCTAG[FAF]*N*CCTC; *N* = G, A, C, or T) (Figure 1a). The hydrogen atom on C7 of AF was replaced with a fluorine atom. The additional base pair was added with InsightII (Accelrys Software, Inc.), using classic B-DNA conformation as a guide. Partial charges in the S conformation were obtained with Gaussian 03 (Gaussian, Inc.) following the standard procedure (*17*). Force field parameters for FAF-dG were obtained by finding the closest analogies in the PARM99 (*18*) and GAFF (*19*) force fields. Molecular dynamics (MD) simulations were carried out with AMBER 8.0 (University of California, San Francisco), employing the modified Cornell et al. force field (*20*).

Substrate Construction and Protein Purification. DNA substrates of 51 bp containing a single FAF or AF adduct with different flanking sequences were constructed as described previously (*21*, *22*). Briefly, the substrates were constructed by ligating a modified 12-mer (CTTCTAG*NCCTC) with a flanking 20-mer (GACTACGTACTGTTACGGCT) and a 19-mer (GCAATCAGGCCAGATCTGC) oligonucleotides on the 5′- and 3′-sides, respectively.

Table 1. Dynamic NMR and Thermodynamic Parameters for the −AG[FAF]*N*− Series Duplexes[a]

	−AG[FAF]G−	−AG[FAF]A−	−AG[FAF]C−	−AG[FAF]T−
% B/S conformation[b]	32/68	39/61	60/40	64/36
$k_{30°C}$ (s^{-1})[c]	200	191	263	200
τ (1/k) (ms)[d]	5.0	5.2	3.8	5.0
k_C[e] = 2.22* $\Delta\nu$[f] (s^{-1})	1214	1202	1240	1715
$\Delta G^{\ddagger}_{30°C}$ (kcal/mol)[g]	14.6	14.6	15.4	14.6
$\Delta G°_{20°C} = \lvert -RT\ln K_{eq}\rvert$ (cal/mol)[h]	439	376	236	334

[a] The trimer core sequence of the −AG[FAF]*N*− series duplexes used in this study, (5′-CTTCTAG*NCCTC-3′) (5′-GAGG*N*CTAGAAG-3′) (*N* = G, A, C, T). [b] Percent population of B and S conformers by integration of ^{19}F NMR signals at 20 °C (SD = ±3%). [c] Rate constants obtained from complete line shape analysis of temperature-dependent ^{19}F NMR spectra using WINDNMR-Pro shareware developed by at the University of Wisconsin at Madison (http://www.chem.wisc.edu/areas/reich/plt/windnmr.htm). [d] Exchange time (1/k) indicates the amount of time the adduct spends in one conformation before jumping into another conformation. [e] Rate constants at a coalescence temperature, which represents a lower limit on the first-order exchange rate between the two conformers. [f] Chemical shift difference between the two signals in Hz at slow exchange, i.e., at 5 °C. [g] S/B interconversion energy barrier in kcal/mol calculated from Eyring equation: $\Delta G^{\ddagger}_{30°C} = 4.58\ T_C\ (10.32 + \log T/k)$ (SD ± 0.2 kcal/mol). [h] Energy difference between the two conformers in absolute values, K_{eq} = S/B.

The 20-mer was 5′-terminally labeled with ^{32}P. The ligation products were purified by urea-PAGE under denaturing conditions. After purification, the ligated 51-mer was annealed with their corresponding complementary strands (bottom 51-mer) and purified again on an 8% polyacrylamide native gel for use.

The UvrA, UvrB, and UvrC proteins were overexpressed and purified from *E. coli* in our laboratory as described previously (*23*). The estimated purity of three proteins was more than 95%. The protein concentration was determined by Bio-Rad protein assay using BSA as a standard following the manufacture's procedures.

Nucleotide Excision Assays. The 5′-terminally labeled DNA substrates (2 nM) were incised by UvrABC (UvrA, 15 nM; UvrB, 250 nM; and UvrC, 100 nM) in the UvrABC buffer (50 mM Tris-HCl, pH 7.5, 50 mM KCl, 10 mM $MgCl_2$, 5 mM DTT, and 1 mM ATP) at 37 °C in a time−course-dependent manner. The Uvr subunits were diluted and premixed into storage buffer before mixing with DNA. Aliquots of the reactions were collected at 0, 5, 10, 15, and 20 min, and the reaction of the aliquots was terminated by adding EDTA (20 mM) or heating to 90 °C for 3 min. The samples were denatured with formamide and heated to 90 °C for 5 min and then quick-chilled on ice. The digested products were analyzed by electrophoresis on a 12% polyacrylamide sequencing gel under denaturing conditions with TBE buffer (*24*).

Quantification of Incision Products. Quantitative data of radioactivity were obtained using Fuji FLA-5000 Image Scanner and Image Gauge V3.46 software and using the volume integration method. The amount of DNA incised (in pmol) by UvrABC was calculated based on the total molar amount of DNA used in each reaction and the percentage of radioactivity in the incision products as compared to the total radioactivity. At least three independent experiments were performed for determination of the rates of incision. The initial rate was determined by a linear least-squares fit of the data collected over the incision period.

Results and Discussion

Figure 1c shows ^{19}F NMR spectra of four 12-mer heteroduplexes modified by the "fluorine reporter probe" FAF (Figure 1a): d(CTTCTAG[FAF]*N*CCTC):d(GAGG*N*CTAGAAG), in which the 3′-flanking base to the lesion is systemically altered (*N* = G, A, C, or T) (*9*). The population of S conformation decreases in the order of 3′-G > A ≫ C > T, indicating the importance of the purine flanking bases in promoting the stacking structure. A S → B interconversion requires a swing of the bulky intercalated carcinogen residue from a *syn*- to an *anti*-glycosidic angle (χ) (Figure 1b). Molecular modeling (Figure 2) indicates that the 3′-flanking G:C base pair of the −AG*G− duplex is broken, which enables the amino protons of 5′-dA_{mod} and 5′-dC_{comp} to form multifurcated hydrogen bondings with the oxygens of the carcinogen-modified dG_{mod}, 3′-dG_{mod} and 3′-dT_{comp}. The highly coordinated hydrogen-bonded structure may stabilize the S conformation relative to the B conformation. The Watson−Crick geometry for the flanking base pairs of the low (36%) S conformeric −AG*T− duplex (Figure 2a), however, resembles that of the unmodified control duplex.

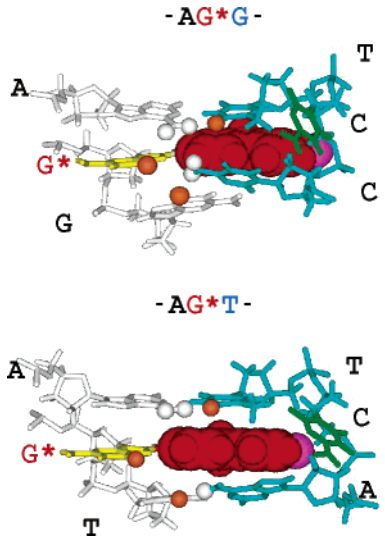

Figure 2. Average structures in the trajectory of the trimer segments for the S conformeric (a) −AG[FAF]G− and (b) −AG[FAF]T− duplexes are shown. Color code: FAF, red-CPK; fluorine, purple CPK; gray, modified (mod) strand; blue, complementary (comp) strand; yellow, FAF-modified G; green, cytosine opposite FAF-modified G; and orange and white balls are oxygens and hydrogens involved in hydrogen bonding, respectively; O^6-G^*_{mod}/5′-$A_{mod-NHnb}$ = 2.8 Å; O^6-3′-G_{mod}/5′-$C_{mod-NHb}$ = 2.1 Å.

Line-shape analysis of temperature-dependent dynamic NMR results (Table 1) showed that all four duplexes follow a typical two-site chemical exchange. The S/B interconversion energy barriers ($\Delta G^{\ddagger}$) are of the order of 14−16 kcal/mol. The energy differences ($\Delta G° = -RT\ln K_{eq}$) of the two conformers are relatively small (<0.5 kcal/mol), suggesting a possibility for facile adduct conformation switch in the active pockets of a protein (*6*, *13*, *25*). Exchange rates at coalescence temperature ($k_C = 2.22 \times \Delta\nu$) were found to be in 1202−1715 s^{-1}, which are faster than those typically observed for spontaneous opening of Watson−Crick base pairs (*26*). Despite the absence of hydrogen bonds, the carcinogenic moiety in the S conformation spends significant time (τ = 3.8−5.2 ms) at 20 °C. The millisecond level S/B exchanges suggest their physiologic accessibility by repair proteins. A similar scenario can be made for a DNA polymerase, rationalizing either error-free or error-prone replication.

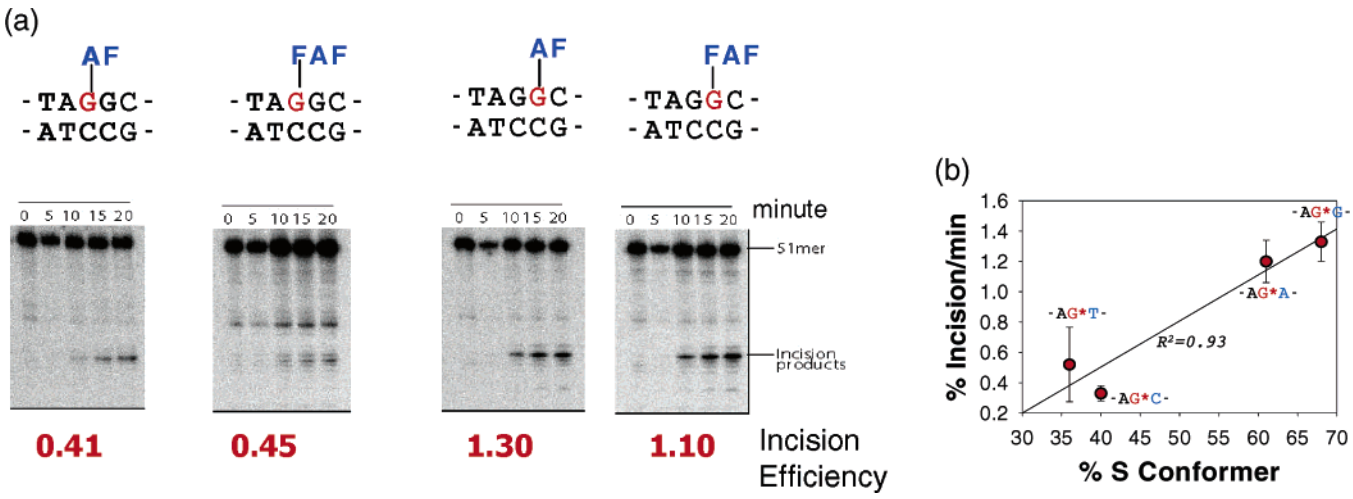

Figure 3. Incision efficiency (%DNA incision/min) of (a) AF and FAF adducts on two different sequences (5′-CTTCTAG*GCCTC-3′ and 5′-CTTCTAGG*CCTC-3′, G* = AF or FAF adduct) and (b) the −AG*N− sequences vs % S conformer by *E. coli* UvrABC nuclease.

It is not known which conformer, S or B, is recognized as a defect in the first step of NER. The S-exclusive AAF adduct is repaired more readily than the AF adduct (*8*, *9*). However, the AF stacking in the S conformation has been shown to be responsible for the thermal and thermodynamic stabilization of a duplex (*14*), which are known negative indicators for NER (*27*). Although the modified dG of B conformer maintains Watson−Crick bonds at the lesion site (Figure 1b), it is possible that the hydrophobic AF moiety in the major groove may create an unfavorable solvation, inducing a greater repair. Figure 3 shows repair results for the aforementioned sequences incised by the *E. coli* UvrABC excinuclease system. Control experiments (Figure 3a) with two different sequences indicated that the incision efficiency is not affected by the presence of fluorine. In addition, the DNA sequence itself should have no intrinsic effect on the incision efficiency as UvrA binds to undamaged DNA nonspecifically or in a sequence-independent manner (*28*). DNA sequence at a lesion may only affect the structure of the lesion, which is recognized and incised by the UvrABC system. Although data are limited, the results in Figure 3b indicate a correlation (R^2 = 0.93) between S conformation and repair. Consistently greater incision efficiencies were observed for high S conformeric −AG*G− (68%) and −AG*A− (61%) sequences. The S conformation, which lacks Watson−Crick base pairs, is also similar to the base-displaced *cis*-benzo[a]pyrene-N^2-dG adducts, which are in contrast with minor groove *trans* adducts with intact Watson−Crick base pairs at the lesion site (*4*, *29*). The study by Zou et al. (*21*) indicated that the base-displaced intercalated adducts are incised by UvrABC more efficiently than the minor groove *trans* adducts. Thus, the growing evidence is that the NER is more efficient for base-displaced intercalated adducts than for adducts in major/minor grooves with intact Watson−Crick hydrogen bonds (*8*, *9*).

Because all of the substrates examined in this study contain the same adduct molecule, FAF, they should be recognized equally well by UvrB (*30*). Thus, the repair results provide valuable insight into the initial recognition of the AF conformational heterogeneity by the $UvrA_2B$ proteins and reinforce the importance of Watson−Crick base pairing for a multipartite model of DNA repair (*27*). Our CD studies showed, however, that neither the B nor the S conformation significantly alters the global conformation of a B-DNA (*12*, *14*). One possibility is an indirect readout mechanism for the local conformational distortion of either the modified (*31*) or the complementary strand (*32*) at the modification site. An alternative scenario is a subtle difference of polarity and shape in the walls of the major groove area: extrusion of the highly hydrophobic AF moiety in B conformer or the highly polar dG and dC at the lesion site in S conformer (Figure 1b).

In conclusion, the ^{19}F NMR/NER data presented in this study lead to an understanding of how bulky DNA adducts are accommodated by the NER protein in a conformationally specific manner. The results represent the first of its kind quantitative structure−function investigation relating fractions of S conformers with increased NER efficiencies, which are the novel aspects of this study.

Acknowledgment. We are grateful to the NIH (R01CA-098296) for their financial support for this work. This research was made possible in part by the use of the RI-INBRE Research Core Facility supported by the NCRR/NIH (P20 RR016457). S.M. and S.M.S. contributed equally to this work.

References

(1) Hoeijmakers, J. H. J. (2001) Genome maintenance mechanisms for preventing cancer. *Nature 411*, 366−374.
(2) Luch, A. (2005) Nature and nature-lessons from chemical carcinogenesis. *Nat. Rev. Cancer 5*, 113−125.
(3) Lukin, M., and de Los Santos, C. (2006) NMR structures of damaged DNA. *Chem. Rev. 106*, 607−686.
(4) Cho, B. P. (2004) Dynamic conformational heterogeneities of carcinogen-DNA adducts and their mutagenic relevance. *J. Environ. Sci. Health, Part C 22*, 57−90.
(5) Heflich, R. H., and Neft, R. E. (1994) Genetic toxicity of 2-acetylaminofluorene, 2-aminofluorene and some of their metabolites and model metabolites. *Mutat. Res. 318*, 73−114.
(6) Hsu, G. W., Kiefer, J. R., Burnouf, D., Becherel, O. J., Fuchs, R. P., and Beese, L. S. (2004) Observing translesion synthesis of an aromatic amine DNA adduct by a high-fidelity DNA polymerase. *J. Biol. Chem. 279*, 50280−50285.
(7) Mekhovich, O., Tang, M., and Romano, L. J. (1998) Rate of incision of N-acetyl-2-aminofluorene and N-2-aminofluorene adducts by UvrABC nuclease is adduct- and sequence-specific: comparison of the rates of UvrABC nuclease incision and protein-DNA complex formation. *Biochemistry 37*, 571−579.
(8) Gillet, L. C. J., and Scharer, O. D. (2006) Molecular mechanisms of mammalian global genome nucleotide excision repair. *Chem. Rev. 106*, 253−276.
(9) Truglio, J. J., Croteau, D. L., Van Houten, B., and Kisker, C. (2006) Prokaryotic nucleotide excision repair: The UvrABC system. *Chem. Rev. 106*, 233−252.
(10) Zhou, L., Rajabjadeh, M., Traficante, D. D., and Cho, B. P. (1997) Conformational heterogeneity of aryl amine-modified DNA: ^{19}F NMR evidence. *J. Am. Chem. Soc. 119*, 5384−5389.

(11) Patel, D. J., Mao, B., Gu, Z., Hingerty, B. E., Gorin, A., Basu, A. K., and Broyde, S. (1998) Nuclear magnetic resonance solution structures of covalent aromatic amine-DNA adducts and their mutagenic relevance. *Chem. Res. Toxicol. 11*, 391−407.

(12) Liang, F., Meneni, S., and Cho, B. P. (2006) Induced circular dichroism characteristics as conformational probes for carcinogenic aminofluorene-DNA adducts. *Chem. Res. Toxicol. 19*, 1040−1043.

(13) Dutta, S., Li, Y., Johnson, D., Dzantiev, L., Richardson, C. C., Romano, L. J., and Ellenberger, T. (2004) Crystal structures of 2-acetylaminofluorene and 2-aminofluorene in complex with T7 DNA polymerase reveal mechanisms of mutagenesis. *Proc. Natl. Acad. Sci. U.S.A. 101*, 16186−16191.

(14) Meneni, S. R., D'Mello, R., Norigian, G., Baker, G., Gao, L., Chiarelli, M. P., and Cho, B. P. (2006) Sequence effects of aminofluorene-modified DNA duplexes: Thermodynamic and circular dichroism properties. *Nucleic Acids Res. 34*, 755−763; 1945 (Erratum).

(15) Friebolin, H. (1998) *Basic One- and Two-Dimensional NMR Spectroscopy*, 3rd ed., pp 301−329, Wiley-VCH, New York.

(16) Mao, B., Hingerty, B. E., Broyde, S., and Patel, D. J. (1998) Solution structure of the aminofluorene [AF]-intercalated conformer of the *syn*-[AF]-C^8-dG adduct opposite dC in a DNA duplex. *Biochemistry 37*, 81−94.

(17) Wang, J. M., Cieplak, P., and Kollman, P. A. (2000) How well does a restrained electrostatic potential (RESP) model perform in calculating conformational energies of organic and biological molecules? *J. Comput. Chem. 21*, 1049−1074.

(18) Cheatham, T. E., III, Cieplak, P., and Kollman, P. A. (1999) A modified version of the Cornell et al. force field with improved sugar pucker phases and helical repeat. *J. Biomol. Struct. Dyn. 16*, 845−862.

(19) Wang, J., Wolf, R. M., Caldwell, J. W., Kollman, P. A., and Case, D. A. (2004) Development and testing of a general amber force field. *J. Comput. Chem. 25*, 1157−1174.

(20) Cornell, W. D., Cieplak, P., Bayly, C. I., Gould, I. R., Merz, K. M., Ferguson, D. M., Spellmeyer, D. C., Fox, T., Caldwell, J. W., and Kollman, P. A. (1995) A second generation force field for the simulation of proteins, nucleic acids, and organic molecules. *J. Am. Chem. Soc. 117*, 5179−5197.

(21) Zou, Y., Liu, T. M., Geacintov, N. E., and Van Houten, B. (1995) Interaction of the UvrABC nuclease system with a DNA duplex containing a single stereoisomer of dG-(+)- or dG-(−)-anti-BPDE. *Biochemistry 34*, 13582−13593.

(22) Yang, Z., Colis, L. C., Basu, A. K., and Zou, Y. (2005) Recognition and incision of gamma-radiation-induced cross-linked guanine-thymine tandem lesion G[8,5-Me]T by UvrABC nuclease. *Chem. Res. Toxicol. 18*, 1339−1346.

(23) Zou, Y., Shell, S. M., Utzat, C. D., Luo, C., Yang, Z., Geacintov, N. E., and Basu, A. K. (2003) Effects of DNA adduct structure and sequence context on strand opening of repair intermediates and incision by UvrABC nuclease. *Biochemistry 42*, 12654−12661.

(24) Luo, C., Krishnasamy, R., Basu, A. K., and Zou, Y. (2000) Recognition and incision of site-specifically modified C8 guanine adducts formed by 2-aminofluorene, *N*-acetyl-2-aminofluorene and 1-nitropyrene by UvrABC nuclease. *Nucleic Acids Res. 28*, 3719−3724.

(25) Seo, K. Y., Nagalingam, A., Tiffany, M., and Loechler, E. L. (2005) Mutagenesis studies on four stereoisomeric N^2-dG benzo[*a*]pyrene adducts in the identical 5′-CGC sequence used in NMR studies: Although adduct conformation differs, mutagenesis outcome does not as G->T mutations dominate in each case. *Mutagenesis 20*, 441−448.

(26) Dornberger, U., Leijon, M., and Fritzsche, H. (1999) High base pair opening rates in tracts of GC base pairs. *J. Biol. Chem. 274*, 6957−6962.

(27) Geacintov, N. E., Broyde, S., Buterin, T., Naegeli, H., Wu, M., Yan, S., and Patel, D. J. (2002) Thermodynamic and structural factors in the removal of bulky DNA adducts by the nucleotide excision repair machinery. *Biopolymers 65*, 202−210.

(28) Van Houten, B. (1990) Nucleotide excision repair in *Escherichia coli*. *Microbiol. Rev. 54*, 18−51.

(29) Geacintov, N. E., Cosman, M., Hingerty, B. E., Amin, S., Broyde, S., and Patel, D. J. (1997) NMR solution structures of stereoisometric covalent polycyclic aromatic carcinogen-DNA adduct: Principles, patterns, and diversity. *Chem. Res. Toxicol. 10*, 111−146.

(30) Zou, Y., Luo, C., and Geacintov, N. E. (2001) Hierarchy of DNA damage recognition in *Escherichia coli* nucleotide excision repair. *Biochemistry 40*, 2923−2931.

(31) Isaacs, R. J., and Spielmann, H. P. (2004) A model for initial DNA lesion recognition by NER and MMR based on local conformational flexibility. *DNA Repair 4*, 455−464.

(32) Buterin, T., Meyer, C., Giese, B., and Naegeli, H. (2005) DNA quality control by conformational readout on the undamaged strand of the double helix. *Chem. Biol. 12*, 913−922.

TX600273H